DOI: https://dx.doi.org/10.4314/gjpas.v30i1.6

GLOBAL JOURNAL OF PURE AND APPLIED SCIENCES VOL. 30, 2024: 51-71
COPYRIGHT© BACHUDO SCIENCE CO. LTD PRINTED IN NIGERIA ISSN 1118 – 0579, e-ISSN: 2992 - 4464
www.globaljournalseries.com.ng, Email: globaljournalseries@gmail.com

INVESTIGATION OF THE INFLUENCE OF THE TURBINE WICKET GATES CLOSURE LAW PATTERN ON THE WATER HAMMER EFFECT DURING TURBINE OFF-DESIGN OPERATION

ROMUALD BAGARAGAZA, FELICIEN MAJORO, JIAN ZHANG, CLAIRE DUSABEMARIYA, RONALDO MUVUNYI, PHILIBERT NSENGIYUMVA, CONCILIE MUKAMWAMBALI, ERIC MBABAZI BUREGEYA, ASSIEL MUGABE AND ADRIEN UWAMAHORO

(Received 16 January 2024; Revision Accepted 6 February 2024)

ABSTRACT

Hydraulic transients are accelerated by the wicket gate closing in hydroelectric power plants. When the wicket gate is closed, there is a sudden change in velocity due to the closure. Therefore, a study has been carried out here, wherein water hammers on different hydropower components use optimum closure laws: Fast closure laws, slow closure laws, and instant load rejection. Hammer V10i software was used to investigate the phenomenon of pressure transient. The results show that the maximum transient pressure is strongly influenced by a very short closing time and was increased to 41.24% from the slow to the fast closure.

Furthermore, the results from instant load rejections reveal that the transient pressure will be less than the fast and slow closure. So, the closing law selection can positively influence the entire hydropower plant system. Furthermore, the results show that there was a decrease in pressure near the turbine during the different load rejections, Fast closure, slow closure, and instant load rejection, where 57.7%, 15%, and 0.46%, respectively, and the decrease in turbine rotation speed were as 5.1%, 60%, and 24% respectively. Moreover, results reveal that maximum and minimum flow variation reached -29.75% and 41.2% during the fast closure.

KEYWORDS: Hydropower plants, Transient flow, Water hammer, Surge tank, Transient pressure fluctuation

7 INTRODUCTION

In water supply and hydropower facilities, a water hammer (WH) is a common occurrence characterized by a sudden increase in pressure inside a pipeline or penstock, corresponding to waves of pressure (acoustics) forming inside the pipe. The phenomenon occurs when the flow in pipes suddenly changes due to three factors: Turbine load rejection and acceptance, The collapse of the vapor pocket, and Rapid airflow from a vent causing water to splash.

This negative effect can be avoided by carefully designing the hydroelectric station based on models. The work is focused on this topic. When pressure and velocity rapidly change in a fluid stream flow system, it is called transient flow (TF) [1]. It is essential to understand that transient Flows can occur in all fluid streams, regardless of their confinement or unconfinement. (WH). It is a sudden change in flow, often caused by an immediate change in flow, like a pipeline, which produces a large transient pressure fluctuation (TPF) [2].

Romuald Bagaragaza, University of Rwanda, College of Science and Technology, Department of Civil, Environmental and Geomatics Engineering, P.O. Box 3900, Kigali, Rwanda
Felicien Majoro, University of Rwanda, College of Science and Technology, Department of Civil, Environmental and Geomatics Engineering, P.O. Box 3900, Kigali, Rwanda
Jian Zhang, Hohai University, College of Water Conservancy and Hydropower Engineering, Jiangsu, Nanjing, 210098, China
Claire Dusabemariya, Protestant Institute of Arts and Social Sciences, Department of Geography, P.O. Box 619, Rwanda
Ronaldo Muvunyi, NPD Ltd and MI Parters, PO Box 495, Kigali, Rwanda
Philibert Nsengiyumva, University of Rwanda, College of Science and Technology, Department of Electronics and Telecommunication, P.O. Box 3900, Kigali, Rwanda
Concilie Mukamwambali, University of Rwanda, College of Education, Department of Mathematics, Science and Physical Education, P.O. Box 55, Rwamagana, Rwanda
Eric Mbabazi Buregeya, Michigan Technological University, Department of Civil, Environmental and Geospatial Engineering, P.O. Box 1400 Townsend Drive, Houghton, Michigan 49931
Assiel Mugabe, Rwanda Polytechnic / IPRC Kigali, Department of Civil Engineering, P.O. Box 3900, Kigali, Rwanda
Adrien Uwamahoro University of Rwanda, College of Science and Technology, Department of Architecture, P.O. Box 3900, Kigali, Rwanda

Two approaches can be used to investigate water hammer: a rigid water column theory that ignores fluid compressibility and a pipe wall elasticity model that integrates pipe movement with fluid compression [3]. When wave speed exceeds 1000 m/s, the pipeline system may suffer severe damage from the pressure waves and high noise. A T.P.F. shifts from very high to very low values when there are different cavitation forms or other serious issues. There are many causes of (WH). However, in most cases, large changes in pressure are caused by four factors: sudden turbine failures during starts or stops (load rejection and acceptance), rapid valve adjustment and instabilities in the turbine, and vibration due to the rotor [4,5]. To ensure that hydraulic systems can support both on and off-design operations, they must be designed to address all of the causes mentioned above [6].

Due to inertia and flexibility, the Water Hammer shock can be increased along the pressurized pipe of the hydropower plant system as well as in water distribution systems. A surge tank chamber and air valves are common equipment to ensure security in hydropower plants with complex operations.[7-10][11].When the continuity of the pressurized pipes is interrupted, the water can quickly be released from its energy, allowing the water level contained in the Surge Tank to rise and fall quickly[12]. Due to the development of computer science, numerical simulation has become the dominant transient analysis method[13]. Different methods have been introduced and implemented to simulate transient phenomena, such as finite-differential and finite-element methods, which have been implemented for transient simulations[14].

Due to its simplicity, the method of characteristics (MoC) is the most commonly used methodology in engineering projects for reproducing the transient process. Nevertheless, the Mac Cormack technique is also applied for solving hyperbolic partial differential equations of free surface flows in dynamic fluids, which are problems associated with partial differential equations[15]. Despite the efforts, simulating the boundary conditions of the device is still quite challenging. Therefore, an attempt should be made to investigate the feasibility of a shock-capturing method within the framework of free-surface flow to achieve convergence of the solutions[16, 17].

Studies have demonstrated how complex devices (C.D.s) can be simplified and retain their original characteristics when lumped together[18]. A system of equations can be used to express the physical characteristics of a simple pipe network. Fang and Chen (2008) developed a simulation system that was able to simulate upstream and downstream S.T.s in a hydroelectric power plant (HPP)[19]. With the help of simplified piecewise linear interface calculations and fluid volume, Zhou and Xu (2018) have shown that hybrid simulations of 3D SP-VOF are efficient, based on a modification of a simulation of a power-off process in pumped storage of hydropower[20].

During water supply systems, T.P.F. is controlled using the S.T. A large part of how well the pressure control system performs can be attributed to the S.T.'s location and size. An S.T. is usually placed near the transient generator to improve pressure control efficiency. As long as the S.T. is not large enough, reducing the T.P.F. effectively will not be possible. Although most applications require a common S.T., a standard S.T. should be sufficient. The positive effects of S.T. throttling on hydraulic transients in hydroelectric power plants (HPP) have been investigated by Vereide and Svingen (2017). This result indicates that throttling can improve T.P. control to a certain degree if applied correctly.

Yang and Wang (2016) developed a mathematical model based on the state-space technique for a tailrace system with an open pipe, utilizing a linear mathematical model for irregular flow [21]. Furthermore, according to their study of water level oscillations, the open tailrace pipe strongly impacts the hydraulic transient process in tailrace S.T. Therefore, a surge relief valve could replace a ST, as Riasi and Tazraei (2017) acknowledge the costs associated with ST construction [22][23]. Skulovich and Bent (2015) used algorithm methods to optimize an ST's position and dimensions to improve transient behavior, and Transient boundaries can be solved using this technique[23]. Solving transient boundaries is possible using this technique. Furthermore, the smooth relationship between tank volume and maximum pressure may influence the selection of protection devices during transient events. Finally, Feng et al. (2017) developed an algorithm that uses bacteria chemotaxis as a multi-objective gravitational search strategy to control the (WH). Pressure and the turbine's rotational speed in a system with two surge tanks positioned on either side of a conveyance line[24]. Wuyi et al. (2019) developed a self-adapting auxiliary control system (SAC) to improve the operating performance and efficiency of surge tanks[10].

This research investigates the negative effects of closing laws on the water hammer pressure in different components of the hydroelectric power plant, including the following parameters: Upstream water tank, penstock-1 Joint-2, Pipe-3 surge tank, tailrace pipe-turbine, and penstock pipe-turbine. In addition, A study was also conducted using Hammer V10i Software to determine the effect of transient flow during turbine instant load rejection, during turbine wicket gate fast closure, and lastly, during turbine wicket gate slow closure. This study was conducted in three scenarios: instant load rejection, slow, and fast closure. Stable conditions are then obtained by applying linear programming optimization in MATLAB. As a result, the water hammer effect is minimized, and pressure

fluctuations are reduced by defining the optimum closure law ranges.

8 METHODOLOGY

Whenever there is an interruption in the system of pipes in a flow system, pressure waves (PW) are produced by the pressure wave propagation. Due to the factors involved in producing pressure waves (PW), TPF changes the flow conditions. Fitting analysis, construction, and design considerations can help avoid these undesirable transient conditions and eliminate the potential for negative PW consequences.

This article analyzes the effects of various wicket gate closure scenarios to minimize the (WH). Problems caused by wicket gate closure scenarios. Several scenarios are used in this article to determine the effectiveness of HAMMER V8i software while reducing the impacts of (WH).

In the first scenario of the turbine with a surge tank, the wicket gate was instantaneously closed, while in the second scenario, the wicket gate was slowly closed. In contrast, in the last scenario, the wicket gate was fast closure. In both closure scenarios, the values of pressure are modeled and compared. In each stage, the different project layout nodes and their effect on the (WH) were piped and compared. A one-dimensional wave equation has been used to develop new mathematical models to evaluate the (WH). The Joukowsky equation correctly predicted maximum line pressures in a hydropower plant system and shock generation times when wicket gates were closed immediately. Hydraulic flow equations have been used to investigate the case of (WH). When a turbine load rejection occurs because of internal pressure. By using the Joukowsky equation, it was possible to calculate any changes in pressure and velocity based on a change in pressure and velocity:

$$\Delta P = \rho a \Delta V \quad \textbf{(1)}$$

Where ρ is water density (kg/m^3), ΔP is the pressure (N/m^2), and ΔV is the velocity change of water in the pipeline (m/s). While a is the velocity (m/s),

$$\Delta H = a\Delta V/g \quad \textbf{(2)}$$

In Eq. (2), g is the gravitational acceleration (m/s2), and ΔH is the pressure variations in terms of water column (m), which is equal to 9.81 m/s^2. As a function of the pipe diameter, the liquid elasticity module, the wall thickness, the pipe material specific weight, and the pressure wave speed are determined by the pipe diameter and liquid elasticity module. Therefore, it is necessary to express the equation of a pressure wave as follows[25]:

$$\text{the } a = \sqrt{\frac{K}{\rho\left(1+\frac{D\pi}{\varepsilon^2 E}\psi\right)}} \quad \textbf{(3)}$$

Where p is the liquid density, E is the pipe elasticity modulus (Young), e is the pipe wall thickness, ψ is a factor related to the pipe supporting condition, and K is the volumetric compressibility modulus of the liquid. Consider the case where one end of the pipe is connected to a bond (RES2), which is filled with water, and on the other end, a valve is installed. A steady-state condition occurs when the flow of water stops abruptly at a time equal to zero (t = 0). In this way, the velocity inside the pipe becomes zero in front of the valve, which causes the water pressure to increase, forcing the pipe diameter to expand simultaneously with the increase in water pressure. This is the moment at which the wave of pressure reaches the bonds [15]

$$T = L/a \quad \textbf{(4)}$$

The pressure wave is reflected at the water's surface during bonding. Water surfaces are considered infinite bodies of constant inertia in the hydraulic view. Consequently, a water surface acts as a solid medium for pressure waves. An unstable situation occurs when reflected waves are found at the transition region between the cross-sectional area of the pipe and where the bond transpires, which causes wave propagation to be unstable. Water starts to flow from the pipe toward the bond after passing the transition region (in the bond). After passing the transition region, the pressure and wave velocity increase, and the wave velocity decreases (flow from high to low pressure). The water body and wave collide. Consequently, pressure energy becomes kinetic energy. The water flows again into the pipe and enters the valve at vibration time, which has the same meaning as the first procedure described above.

$$T = 2L/a \quad \textbf{(5)}$$

Where L is the pipeline length (m), using the equation below, we can determine water velocity:

$$V = Q/S \quad \textbf{(6)}$$

$$S = (\pi D^2)/4 \quad \textbf{(7)}$$

Where D is the pipe diameter (m), and S is the pipe's cross-sectional area. Many factors contribute to head losses in a network pipe system. Internal friction between moving liquid particles is usually the main cause of head loss. Turbulence and interruptions of the streamlines are secondary causes of head loss, such as interruptions caused by valves and other fittings in the pipe pressure or disruptions caused by changing section areas in a network. There are two types of head loss: steady-state losses (H Static) and transient losses (water hammer, h). Based on empirical relationships, the Hazen-Williams formula calculates the head loss (m) over the length of a pipe caused by friction. This relationship relates water flow in the pipe with physical properties and pressure drop.

$$h_f = \frac{10.67^{*}L^{*}Q^{1.852}}{C^{1.852}D^{4.8704}} \quad (8)$$

$$Hmax = H\ \text{static} + h(\ \text{hammer}\ ) + hf \quad (9)$$

Where h_f represents the head loss (m), C represents the pipe roughness coefficient, L represents the length of pipe (m), and Q represents the volumetric flow rate (m^3/s). The value is usually considered a fixed value for specific materials. However, as shown in Table 1, c values vary depending on the pipe material.

9 CASE STUDY

The model consists of a series of reservoirs that are connected. Besides the surge tank and turbine, the network includes pipes (P-1 -P-2), penstock-1 and penstock-2, junctions (J1-J2), and a final tailrace. D/S Reservoir has the lowest water level of 383 meters, and the U/S Reservoir has an elevation difference of 73 meters. In total, there are 1.857 kilometers of pipe in the system. 18 m^3/s is the net volumetric flow of water.

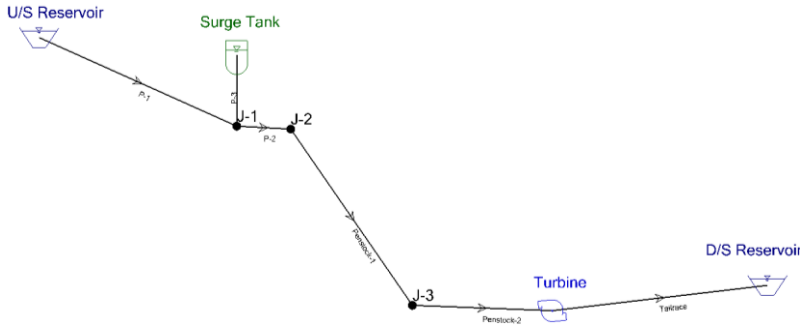

Figure 1: H.E.P.P. Layout

Table 1 presents the study data inventory, and Table 3 shows the main network characteristics. In addition, Table 1 below shows the elevations of the pipelines at the inlet and outlet of the pipes. Finally, the basic characteristics of the turbine, the surge tank, pipes, and reservoirs are described in this paper.

Table 1: Network parameters characteristics

Label	Length (m)	Start Node	Stop Node	Diameter (mm)	Material	Hazen-Williams C	Wave Speed (m/s)
P-3	155.08	J-1	Surge Tank	1000	Concrete	110	1080
P-2	117.76	J-1	J-2	3400	Concrete	110	1080
Penstock-2	304.97	J-3	Turbine	2350	Steel	100	1215
Tailrace	472	Turbine	R-2	3500	Concrete	110	1080
Penstock-1	465.9	J-2	J-3	2350	Steel	100	1215
P-1	471.56	R-1	J-1	3400	Concrete	110	1080

Table 2: Surge tank

Label	Elevation (m)	Diameter (m)	Diameter (Orifice) (mm)	Elevation (Initial) (m)	Elevation (Base) (m)	Elevation (Maximum) (m)	Elevation (Minimum) (m)
Simple Surge Tank	2270	6	1000	2357	2270	2375	2271.1

Table 3. Turbine parameter input

Elevation (m)	Efficiency (%)	Moment of Inertia (N·m²)	Diameter (Spherical Valve) (mm)	Report Period (Transient)	Speed (Rotational) (rpm)	Time (Delay until Valve Operates) (sec)
1714.9	90	10000000	1499.62	10	580	999

Table 3 shows the typical input for the turbine-related electrical torque curve during hydraulic transient operation. The moment of inertia is also an input, and that parameter is when entering the value of the turbine, the generator, and the entrained water.

Table 4: Turbine electrical torque curve

Sn	Time (sec)	Torque(N*m)
1	1	1355000
2	20	1355000
3	21	0
4	30	0

1.1. Simulation procedures of hydro network

Transient analysis in this hydropower system was performed in this research. The evaluation of the system response for four different turbine conditions was carried out, including run-away speed, fast closure of wicked gates, slow closure of wicked gates, and the opening of wicked gates when the turbine starts up or during load rejections. As shown in the

Table *2*, the surge tank is almost 500 meters above the turbine. Therefore, a spherical valve will not be operating during the simulation, which is only 150 seconds, and time to 999 seconds was set to ensure that this valve remains open. During the simulation, the turbine operating case was changed for each scenario, but the other physical properties were kept the same: turbine diameter, efficiency, moment of inertia, etc.

10 RESULT AND DISCUSSION

1.2. Investigation of transient flow at the upstream reservoir

1.2.1. Effect on flow variation during T.F.

For the first scenario, the aim was to create a run-away speed check. This simulation aimed to determine the maximum speed reached by the turbine when the electrical load in the turbine drops instantaneously to zero, creating an initial setting alternative for the turbine to open and a new transient child alternative called instant load rejection. During this scenario, the wicket gates start operating a hundred percent open and are closed after 200 seconds; the simulation lasts only 150 seconds, so the wicket gate will always be open.

The instant load rejection scenario's outcome reveals no user notifications since no transient was expected as the wicket gates stayed open. However, when the speed increases as the electrical load is rejected, the turbine's efficiency changes, leading to choking and a decrease in the flow, as shown in the figure.

Nomenclature

Nomenclature			
a	Speed of pressure wave (m/s)	s	Cross area (m2)
C	Roughness coefficient	S.T.	Surge tank
CD	Complex device	T.P.F.	Transient pressure fluctuation
D	Pipe diameter (m)	V	Flow velocity (m/s)
Ep	elasticity modules of pipe material	(WH).	Water hammer
E	Compression elasticity modules of water	ΔH	Change in head loss
g	Acceleration of gravity (m/s2)	ΔP	Change n pressure (kPa)
h	Pressure head (m)	Δv	change of velocity (m/s)
HPP	Hydroelectric power plant	π	Constant
J	Junction	ρ	Density (kg/m")
L	Length of pipe (m)	τ	The thickness of pipe (m)
P.W.	Wave velocity (m/s)	s	Cross area (m2)

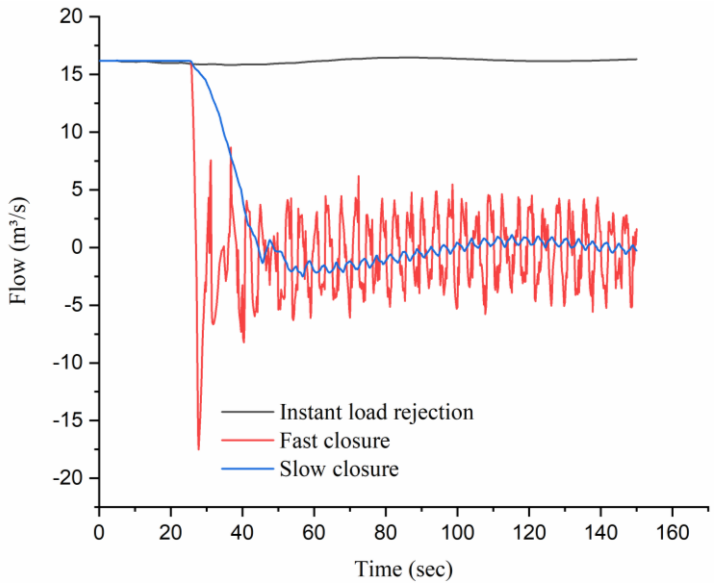

Figure 2: Flow fluctuation in the upstream tank during transient flow

Table 5: Min and Max flow during transient flow

Flow (m³/s)	Standard Deviation	Harmonic Mean	Minimum	Maximum
Instant load rejection	0.18491973	16.16612542	15.82	16.47
Fast closure	7.099829376		-17.52	16.2
Slow closure	6.792660387	0	-2.51	16.2

1.2.2. Effect on velocity during T.F.

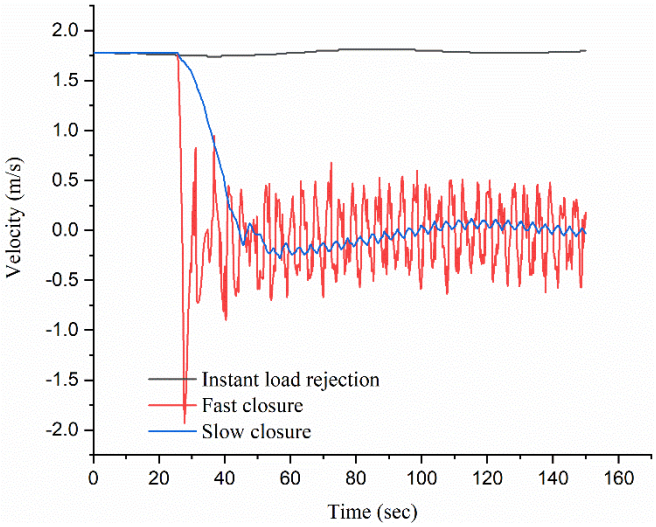

Figure 3: Velocity fluctuation in the upstream tank during transient flow

Table 6: Min and Max Velocity during transient flow

Velocity (m/s)	Standard Deviation	Minimum	Maximum
Instant load rejection	0.020271745	1.74	1.81
Fast closure	0.78120657	-1.93	1.78
Slow closure	0.747483516	-0.28	1.78

1.2.3. Effect on speed during T.F.

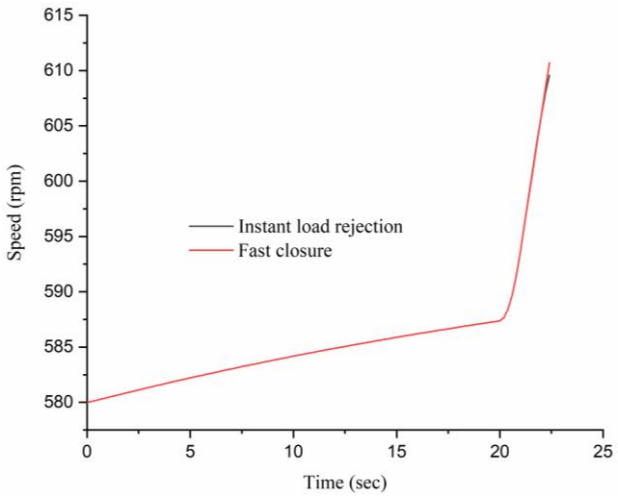

Figure 4: Turbine speed fluctuation during transient flow

Table 7: Min and Max speed during transient flow

Speed (rpm)	Standard Deviation	Skewness	Minimum	Maximum
Instant load rejection	5.333977704	2.723514572	580	609.59
Fast closure	50.26263204	0.853076958	580	721.29

1.2.4. Turbine wicket gate position

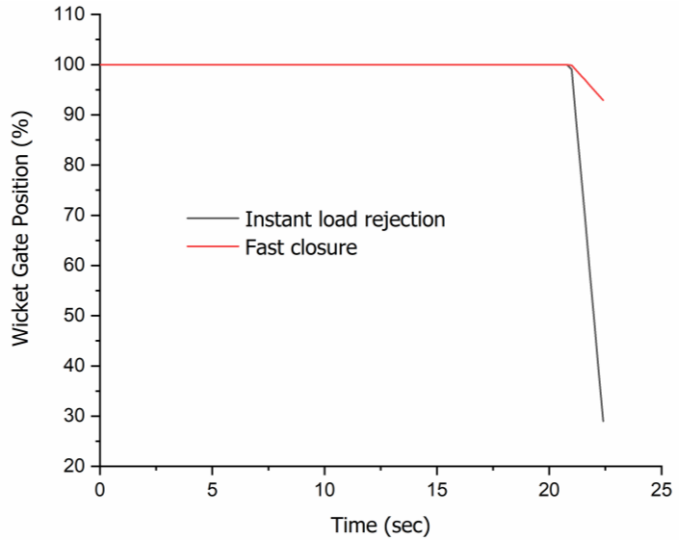

Figure 5: Wicket gate position during load rejection

Nevertheless, it was seen during the evaluation of the turbine's speed that the maximum speed was achieved during this simulation. So, when the maximum speed is achieved and the system becomes stable, it happens for about 120 seconds and is observed to be (951 rpm) as a run-away speed, as shown in Figure 4.

Table 8: Min and Max opening angle of the wicket gate during transient flow

Wicket Gate Position (%)	Standard Deviation	Minimum	Maximum
Instant load rejection	11.11385168	29	100
Fast closure	24.87609955	20.9	100

1.3. Investigation of transient flow at Penstock-1 J-2

1.3.1. Effect on hydraulic grade line

For load rejection fast closure, consider that the electrical load is rejected at the 20s and that the wicket-gate will **close at** 22s. It will take 2s to close the wicket gates completely.

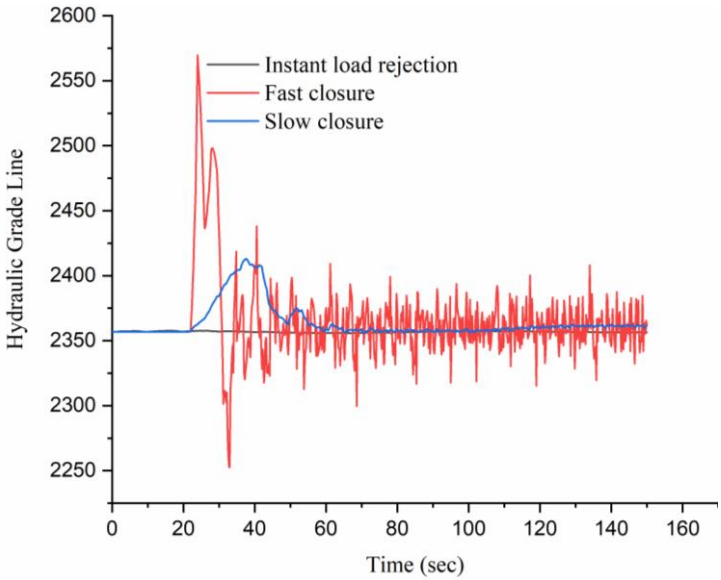

Figure 6: Effect of the hydraulic transient in the penstock

Table 9: Min and Max hydraulic grade line in three scenarios during transient flow

Hydraulic Grade Line	Standard Deviation	Minimum	Maximum
Instant load rejection	0.501121991	2355.84	2357.78
Fast closure	33.08729818	2252.62	2569.75
Slow closure	13.10288056	2355.82	2412.87

Notice the upsurge pressure and the nodes reaching vapor pressure - 97.9. Glimpse that there are many user notifications about cavities opening and closing at J-1 and J-2. Plot the surge tank to the R2 profile for hydraulic grade and air or vapor volume. At about 22 seconds, the pressure up streams of the turbine spiked due to the wicket gate's sudden closure. As the pressure increases, the surge tank starts to fill; at about 29 seconds, the surge tank starts to drain as the pressure drops; however, flow is restricted, and it cannot get to Joint 1 and 2 soon enough to prevent vapor pocket formation.

1.3.2. Effect on pressure variation during T.F.

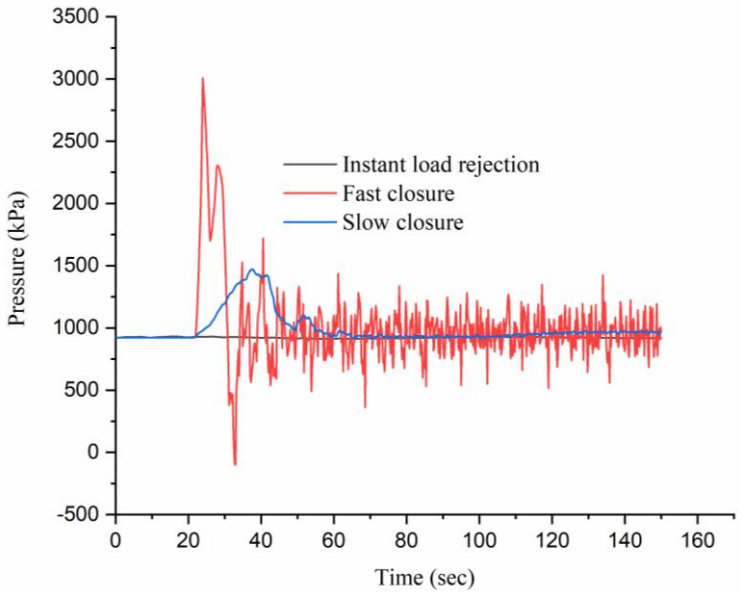

Figure 7: Pressure variation in the penstock during transient flow

Table 10: Min and Max pressure in three scenarios during transient flow

Pressure (kPa)	Standard Deviation	Minimum	Maximum
Instant load rejection	4.906498241	912.5	931.6
Fast closure laws	323.8227976	-97.7	3006
Slow closure claw	128.2351684	912.3	1470.6

The maximum difference between the three scenarios is around 1.8 in terms of transient pressure calculation. Based on these factors, and considering this is a significant one that could damage the system due to high pressure,

Table *10* gives the maximum and minimum pressures.

1.3.3. Effect on flow variation during T.F.

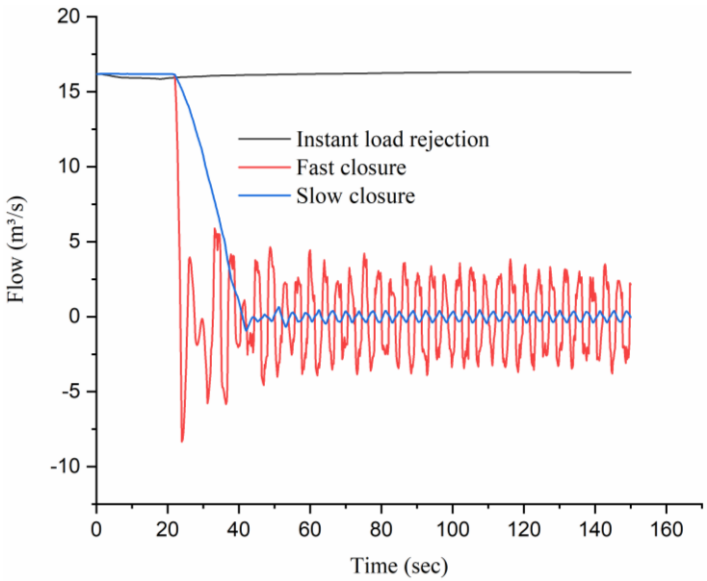

Figure 8: Flow variation in the penstock during transient flow

Table 11: Min and Max flow of three scenarios during transient flow

Flow (m³/s)	Standard Deviation	Minimum	Maximum
Instant load rejection	0.130517862	15.85	16.3
Fast Closure	6.342192794	-8.34	16.19
Slow closure	6.279571091	-0.95	16.19

1.3.4. Effect on velocity during T.F.

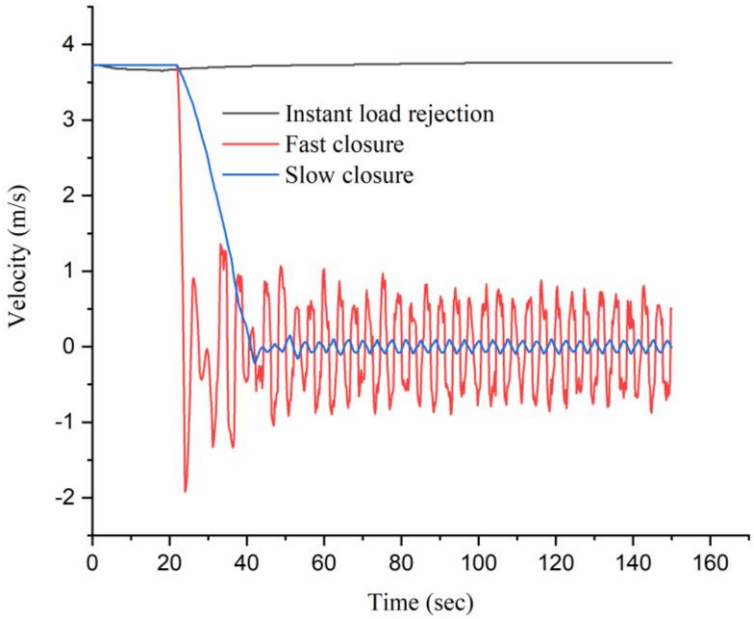

Figure 9: Velocity variation in the penstock during transient flow

Table 12: Min and Max flow velocity of three scenarios during transient flow

Velocity (m/s)	Standard Deviation	Minimum	Maximum
Instant load rejection	0.031080166	3.65	3.76
Fast closure	1.462098276	-1.92	3.73
Slow closure	1.44774988	-0.22	3.73

1.3.5. Effect on speed during T.F.

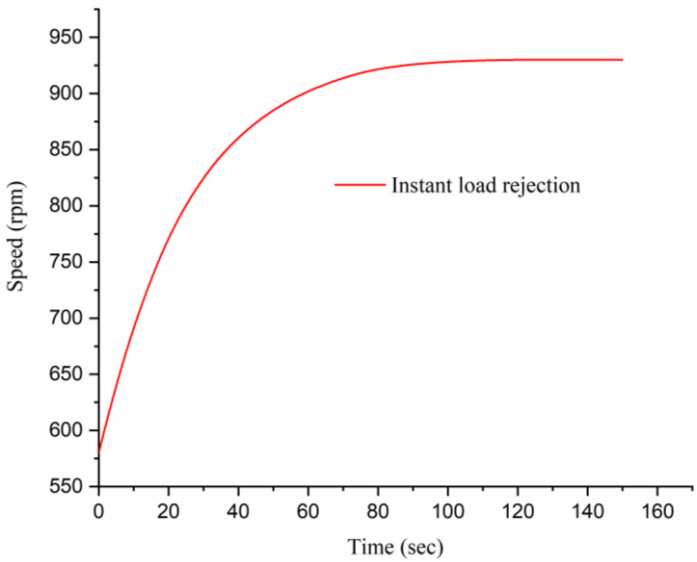

Figure 10: Maximum turbine speed rotation speed during load rejection

Table 13: Min and Max runner speed of three scenarios during transient flow

Speed (rpm)	Standard Deviation	Minimum	Maximum
Fast closure	85.35784472	580	930.19

At j2, notice that a vapor pocket forms and then collapses when the pressure drops below the vapor pressure. What happens near the surge tank for both the pressure head and flow? Notice that following the closure of the wicked gates, the pressure spikes, and the flow goes towards the surge tank, and then at about 29 seconds, it starts to drain. Please note the maximum rotational speed we are getting on this runway for the turbine speed.

1.4. Investigation of transient flow at P-3 Surge tank

1.4.1. Effect on hydraulic grade line

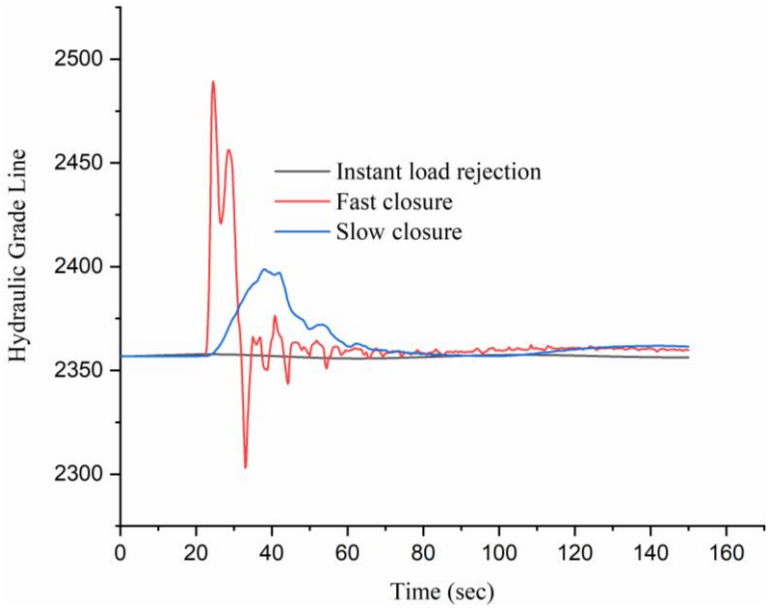

Figure 11: Effect of the hydraulic transient in the in-surge tank

Table 14: Min and Max hydraulic grade line of three scenarios during transient flow

Hydraulic Grade Line	Standard Deviation	Minimum	Maximum
Instant load rejection	0.60072304	2355.74	2357.78
Fast closure	19.88724812	2302.96	2489.28
Slow closure	10.25791112	2356.86	2398.8

Load rejection slow closure with the turbine is open in initial settings, and the time takes two seconds to close. The turbine was slowly closed and took 20 seconds to close. The extreme pressure head observed that the largest ratio is one point five nine, which means the maximum pressure is one point five nine times the steady-state pressure.

The pressure profile from the surge tank to the reservoir R2 reveals that no vapor pockets are forming or collapsing in the slow closure scenario, and the maximum and minimum transient heads are less critical than in the fast closure scenario.

A comparative study of pressure at j-1 between the slow closure and fast closure in time histories reveals that increasing the closure time from two to twenty seconds could prevent vapor pockets from forming, and the high pressures are minimized. Furthermore, the speed of the turbine reveals the maximum rotational speed achieved in this scenario.

1.4.2. Effect on pressure variation during T.F.

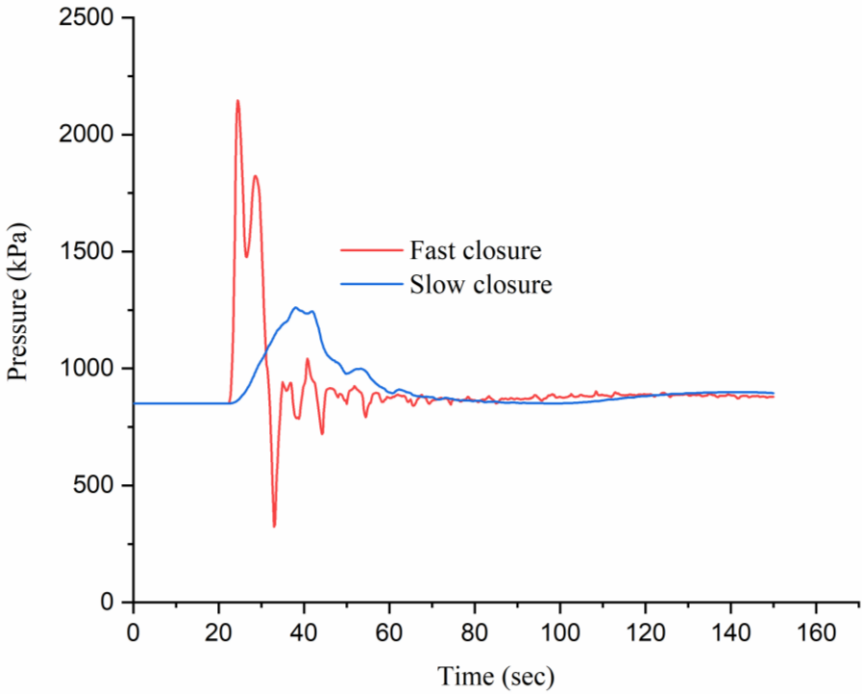

Figure 12: Pressure variation in the surge tank during transient flow

Table 15: Min and Max pressure of three scenarios during transient flow

Pressure (kPa)	Standard Deviation	Minimum	Maximum
Fast rejection	194.6324777	322.6	2146.1
Slow closure	100.3955955	850	1260.6

The maximum difference between the three scenarios is around 1.8 in terms of transient pressure calculation. Based on these factors, and considering this is a significant one that could damage the system due to high pressure, Table 16 gives the maximum and minimum pressures.

1.4.3. Effect on flow variation during T.F.

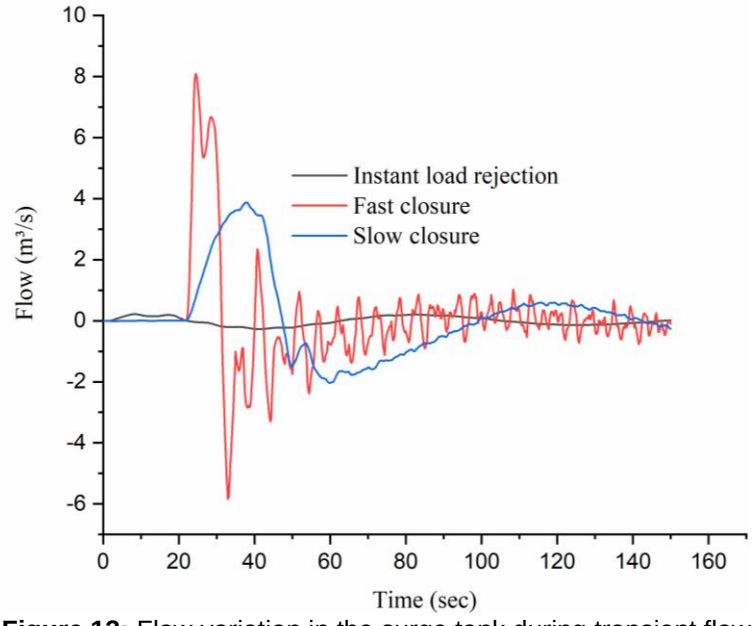

Figure 13: Flow variation in the surge tank during transient flow

Table 16: Min and Max flow of three scenarios during transient flow

Flow (m^3/s)	Standard Deviation	Minimum	Maximum
Instant load rejection	0.141302815	-0.27	0.22
Fast rejection	1.696855203	-5.84	8.09
Slow rejection	1.34999256	-2.03	3.87

1.4.4. Effect on velocity during T.F.

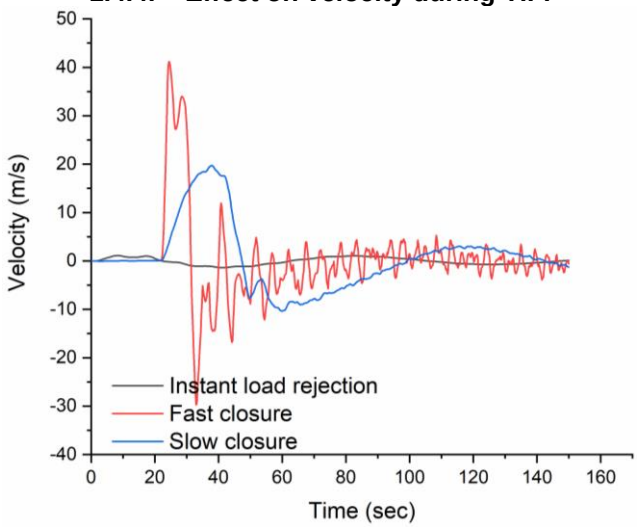

Figure 14: Velocity variation in the surge tank during transient flow

Table 17: Min and Max flow velocity of three scenarios during transient flow

Velocity (m/s)	Standard Deviation	Minimum	Maximum
Instant load rejection	0.719984059	-1.39	1.11
Fast closure	8.642283839	-29.75	41.2
Slow closure	6.874912789	-10.34	19.7

1.5. Investigation of transient flow at tailrace turbine

4.4.4. Effect on hydraulic grade line

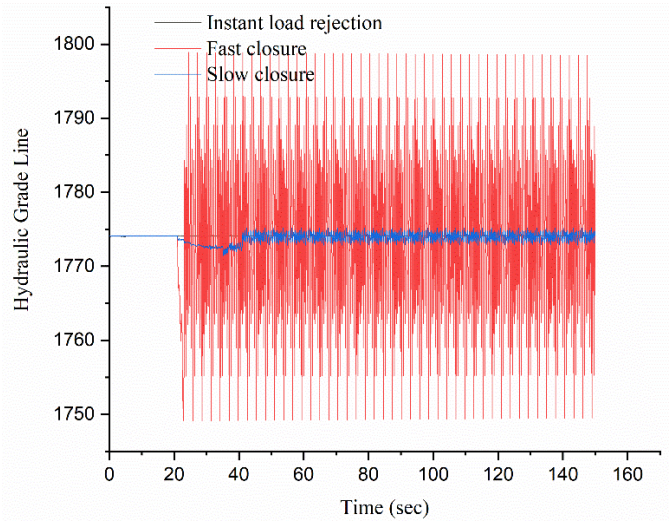

Figure 15: Hydraulic grade line variation at tailrace turbine T.F.

Table 18: Min and Max hydraulic grade line of three scenarios during transient flow

Hydraulic Grade Line	Standard Deviation	Minimum	Maximum
Instant load rejection	0.015273486	1774	1774.13
Fast closure	13.62096236	1749.1	1798.9
Slow closure	0.772941129	1771.42	1775.15

1.5.1. Effect on pressure variation during T.F.

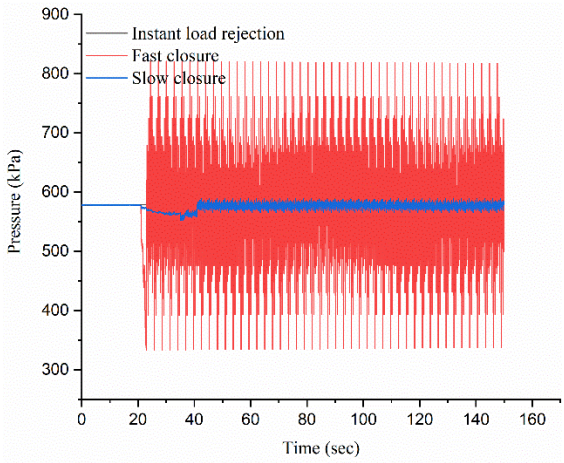

Figure 16: Pressure variation in the tailrace turbine during transient flow

Table 19: Min and Max pressure variation of three scenarios during transient flow

Pressure (kPa)	Standard Deviation	Minimum	Maximum
Instant load rejection	0.149633907	577.4	578.7
Fast closure	133.3019667	333.7	821.1
Slow closure	7.572747961	552.2	588.7

The maximum difference between the three scenarios is around 1.8 in terms of transient pressure calculation. Based on these factors, and considering this is a significant one that could damage the system due to high pressure, Table 10 gives the maximum and minimum pressures.

1.5.2. Effect on flow variation during T.F.

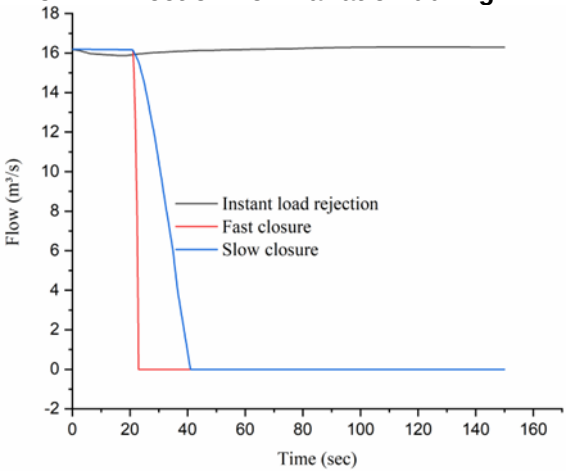

Figure 17: Flow variation resulted from the wicket gate closure

Table 20: Min and Max flow variation of three scenarios during transient flow

Flow (m^3/s)	Standard Deviation	Minimum	Maximum
Instant load rejection	0.130078112	15.87	16.3
Fast closure	5.721875607	0	16.19
Slow closure	6.248720842	0	16.19

1.5.3. Effect on velocity during T.F.

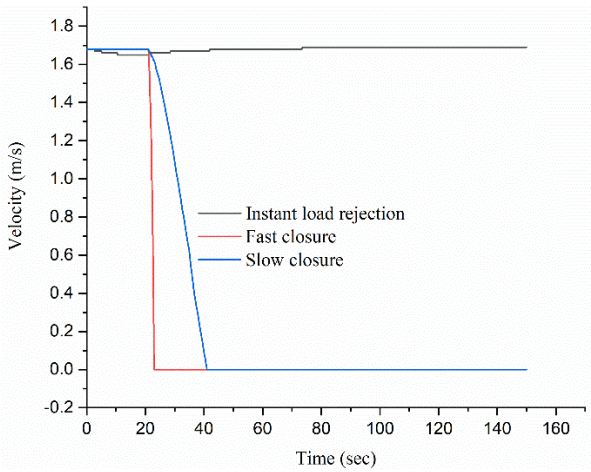

Figure 18: Velocity variation resulted from the wicket gate closure

Table 21: Min and Max flow velocity of three scenarios during transient flow

Velocity (m/s)	Standard Deviation	Minimum	Maximum
Instant load rejection	0.012620698	1.65	1.69
Fast closure	0.594136287	0	1.68
Slow closure	0.649006463	0	1.68

1.6. Investigation of transient flow at penstock-2 turbine

Usually, the wicket gate is used for a turbine for flow regulation. So, the wicket gate is usually what a turbine uses to control the flow through it, and therefore, usually, a governor is constantly monitoring the turbine speed and closing and opening those wicked gates to control the inflow. The wicket gates are modeled as a pattern of relative closures, so the hammer is usually used to see the effects of opening or closing the wicket gate in response to some events.

1.6.1. Effect on hydraulic grade line

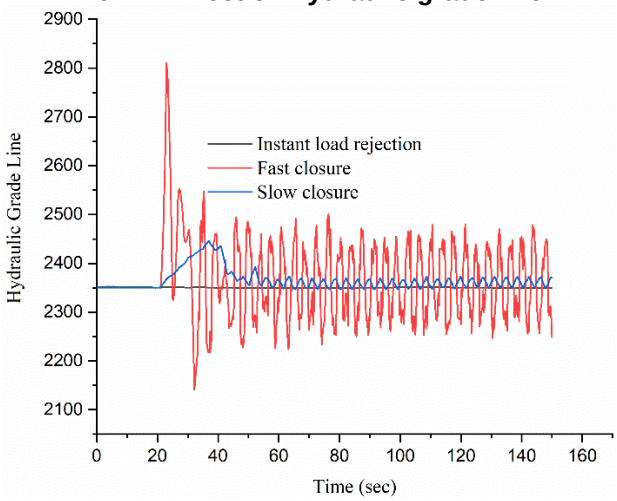

Figure 19: Fluctuation of the Hydraulic grade line at penstock-2 turbine during T.F.

Table 22: Min and Max hydraulic grade line of three scenarios during transient flow

Hydraulic Grade Line	Standard Deviation	Minimum	Maximum
Instant load rejection	0.643280528	2349.2	2352.13
Fast closure	82.74839978	2140.87	2810.51
Slow closure	21.15515266	2346.22	2445.42

1.6.2. Effect on pressure variation during T.F.

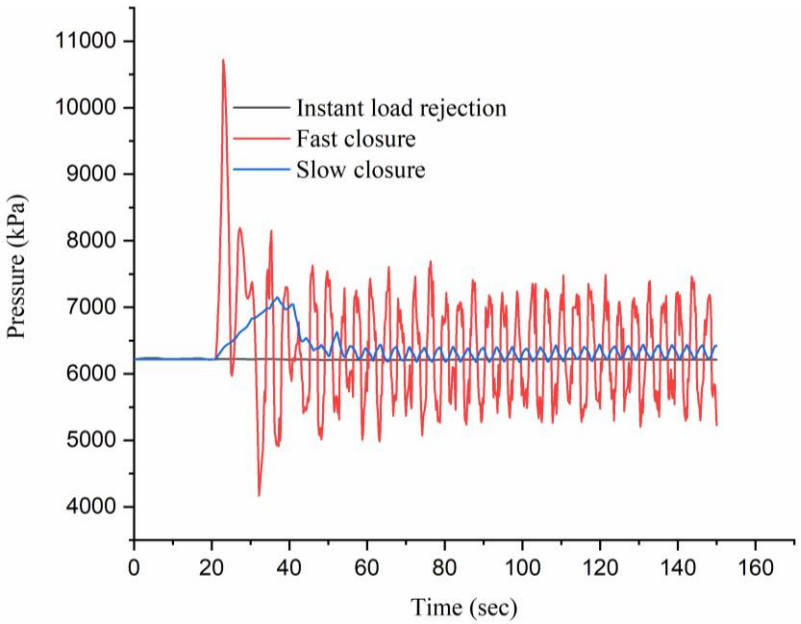

Figure 20: Fluctuation of the pressure at penstock-2 turbine during T.F.

Table 23: Min and Max pressure of three scenarios during transient flow

Pressure (kPa)	Standard Deviation	Minimum	Maximum
Instant load rejection	6.293837001	6206.8	6235.5
Fast closure	809.8472869	4167.9	10721.6
Slow closure	207.0433966	6177.7	7148.5

The maximum difference between the three scenarios is around 1.8 in terms of transient pressure calculation. Based on these factors, and considering this is a significant one that could damage the system due to high pressure, Table 10 gives the maximum and minimum pressures.

1.6.3. Effect on flow variation during T.F.

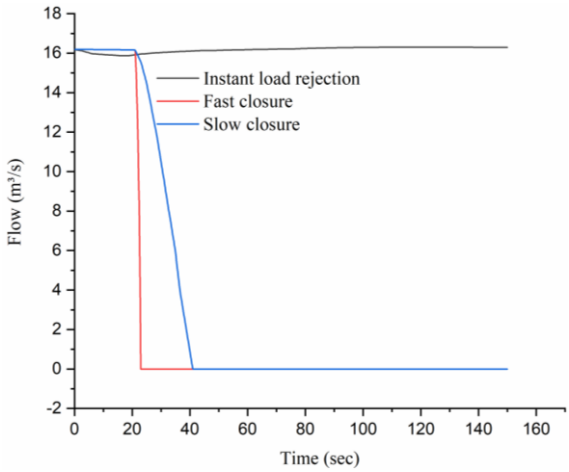

Figure 21: Flow fluctuation at penstock-2 turbine during T.F.

Table 24: Min and Max flow variation of three scenarios during transient flow

Pressure (kPa)	Standard Deviation	Minimum	Maximum
Instant load rejection	6.293837001	6206.8	6235.5
Fast closure	809.8472869	4167.9	10721.6
Slow closure	207.0433966	6177.7	7148.5

Table 25: Min and Max turbine speed of three scenarios during transient flow

Speed (rpm)	Standard Deviation	Minimum	Maximum
Instant load rejection	85.35784472	580	930.19
Fast closure	5.333977704	580	609.59
Slow closure	50.26263204	580	721.29

Instant load rejection, so the assumption is that a turbine operates normally; water flows through it and generates electricity. Therefore, what happened was to simulate a sudden change in the electrical load on the turbine. Instantly, it is reduced to zero, so something happens on the electrical, and suddenly, there is no more electrical load on that turbine, which means the turbine will continue to speed up. Furthermore, it will finally reach the run-away speed, which means the turbine is spinning so fast from all that water flowing through it without the resistance from the electrical load that it could damage itself. Bad things could happen.

The load rejection assumption is an instant drop in the electrical load. Load rejection checking to see what happens if we do not close the wicket gates and what run-away speed will be achieved. During load rejection, we can see that when the load is rejected, the turbine speeds up until it reaches about 930 rpm at about 110 seconds. Therefore, if we compare that to the original of about 580 rpm, there is quite a large difference, which could be a problem.

Fast closure load rejection. If we look at the results, we can see that we have some vapor pocket problems, so the first 20 seconds is when the wicked gates are about to be fully closed. After that, a high-pressure spike results from that transient event that propagates upstream reflux comes back and eventually drops below the vapor pressure limit. We have some vapor forming at about 33, 32 seconds, which collapses, and we eventually reach a final steady state, not quite. However, towards the end, a steady state was reached. There is probably zero flow at this point, and because of that, there is not

much friction to dampen that surge. The wicket gate is slowly closed. For example, the pattern closes the wicket gates between 21 and 23 seconds and closes in about two seconds.

In contrast, the slow closure scenario closes it in about 20 seconds. Hence, if we look at when the wicket gate is closed, there is a much smaller water hammer effect during this scenario, which is much better. In conclusion, closing the wicket gate much slower will significantly impact the transient response.

5. DISCUSSIONS

For the turbine runway speed, the aim was to determine the maximum speed reached when the turbine's electrical load drops instantaneously to zero. Wicket gates will start a hundred percent open and close at 200s, and the simulation only lasts 150s, so the wicket gate will always be open. In brief, there were no vapor pressure formations for the instant load closure scenario since no transient was expected as the wicket gates stayed open. However, when checking the point close to the turbine, it has been shown that when the speed increases as the electrical load is rejected, there is a change in the unit's efficiency, leading to choking and a decrease in the flow, as shown in Figure 22. During the scenario, we also evaluated the maximum speed achieved during this simulation and noticed that the maximum speed happened at about 120 seconds and was 930.18 rpm.

Fast closure usually results in the most severe transient pressures during load rejection. In this scenario, the electrical load is rejected at the 20s, and the wicket gate will start closing at 22s; it took 2s to close the gates completely. There was an upsurge in pressure, and some nodes reached vapor pressure - 75.9, as shown in Table 12. Moreover, there were many notifications about cavities opening and closing, especially at Joint -1 and Joint -2. What happened to the surge tank? Notice that at about 22s, the pressure upstream of the turbine spikes as a result of the wicked gate's sudden closure, and the pressure increases the surge tank at the same time surge tank starts to fill while at about 29s, the surge tank starts to drain as the pressure drops as shown in figure 13 and table 16. however, flow is restricted, and it cannot get to Joint -1 and Joint -2 soon enough to prevent vapor pocket formation, as shown in Figure 14 and Table 16. Investigation at Joint -2 penstock reveals that when the pressure drops below the vapor pressure, a vapor pocket forms and then collapses, as shown in Figures 9 and 21 and Table 12, after observation about what happens near the surge tank in terms of head and flow. Results reveal that following the closure of the wicked gates, the pressure spikes, and the flow goes towards the surge tank, and then at about 29s, it starts to drain, as shown in figures 13 and 14 in tables 16 and 17. For the turbine's maximum rotational speed observed during fast load, rejection ranged to 609.59 rpm, as shown in Figure 4 and Table 7 and 25

During slow load rejection, this time, instead of taking 2 seconds to close, the turbine closed slowly and took 20 seconds to close completely. Results about pressures and heads reveal that the upsurge ratio is about 1.59, which means the maximum pressure is 1.59 times the steady-state pressure. When we analyze the profile of the surge tank to reservoir 2, results reveal that during the slow closure, no vapor pockets are forming or collapsing, and the maximum and minimum transient head envelopes are less critical than in the fast closure scenario.

This analysis compared different parameters from different closing scenarios, and slow, fast, and instant load rejections were compared. The results reveal that the system could prevent vapor pockets from forming by increasing the pressure for closing time from 2s to 20s. Also, the high pressures were minimized, as shown in Figures 7, 13, 17, and 21. The maximum rotational speed achieved during the slow closure was about 721.29 rpm. Table 23 summarizes the three speeds achieved during this investigation. As was noticed, the speed is maximum during the turbine's slow closure, and the speed is minimum during the slow turbine closure.

Upon comparing the two tables representing pressure values (in kPa), standard deviation, minimum, and maximum for Instant Load Rejection, Fast Closure, and Slow Closure scenarios, it is evident that the MATLAB simulation results closely align with those obtained from Bentley Hammer. For Instant Load Rejection, the standard deviation, minimum, and maximum pressures in the MATLAB simulation are slightly lower by approximately 1%, indicating a minor deviation within an acceptable range. In the case of Fast Closure, the MATLAB simulation yields values that are nearly identical to Bentley Hammer results, with a negligible difference of around 0.7%. Similarly, for Slow Closure, the MATLAB simulation results are within approximately 0.5% of Bentley Hammer values. These subtle variations suggest a consistent trend, reinforcing the reliability of the MATLAB simulation in accurately capturing hydraulic behaviors.

The MATLAB simulation consistently demonstrates good agreement with Bentley Hammer results across various scenarios, including Instant Load Rejection, Fast Closure, and Slow Closure. The slight discrepancies observed in pressure values remain within an acceptable range, affirming the reliability of the MATLAB simulation as a robust alternative for hydraulic analysis. This concordance between the two methods establishes the viability of MATLAB for simulating hydraulic phenomena in the given context.

To enhance confidence in the MATLAB simulation's accuracy, it is recommended to conduct further validation against real-world data or additional hydraulic analysis software. This validation process ensures that the MATLAB model accurately represents the dynamic behavior of the hydropower

plant under different conditions. Additionally, continuous monitoring and calibration of simulation tools are crucial to maintaining the reliability of hydraulic analyses across diverse scenarios. Regular updates and adjustments based on observed system behavior contribute to the accuracy and effectiveness of the simulation model over time.

The comparative analysis underscores the potential of MATLAB simulation as a cost-effective and accurate tool for hydraulic analysis in hydropower plant design and operation. Leveraging the consistency observed with Bentley Hammer results, MATLAB proves to be a valuable asset in decision-making processes within the field, offering efficiency and reliability in hydraulic simulations.

6. CONCLUSIONS

Studying the effects of water hammer (H.W.) is crucial for various applications, including gas transportation, long-distance water supply, and hydroelectric power plants. In this study, the impact of water hammer in a hydropower system equipped with a surge tank was investigated using HAMMER V8i software. The analysis considered parameters such as instant load rejection, load acceptance, wicket gate fast close, and slow closure. The results demonstrated that the choice of closing law patterns significantly influences the water hammer phenomenon, with fast closure inducing a more severe effect compared to slow closure. This emphasizes the importance of selecting appropriate closing patterns to mitigate water hammer risks in hydropower plants.

Transient analysis for hydraulic turbines is essential for risk reduction in hydropower projects. The study highlighted the complexity of transient hydraulics and emphasized the need to address hydraulic transient problems promptly. The use of HAMMER V10i, with its advanced functionality and turbine simulation abilities, was deemed crucial for accurately simulating hydraulic transients and ensuring the system's resistance to excessive pressure. The study revealed that transient pressure during instant load rejections was lower than during fast and slow closures, showcasing the positive influence of closing law selection on the entire hydropower plant system. Additionally, an increase in closing time was associated with a decrease in total pressure, underlining the importance of optimizing closing patterns for system stability.

Further insights were gained from the results of different load rejections (fast closure, slow closure, and instant load rejection). A decrease in pressure near the turbine was observed, with significant reductions of 57.7%, 15%, and 0.46% during fast closure, slow closure, and instant load rejection, respectively. The corresponding decrease in turbine rotation speed was 5.1%, 60%, and 24%, suggesting that shorter closing patterns lead to more severe pressure increases and decreased turbine speed.

Moreover, the study highlighted flow variations during fast closure, with maximum and minimum variations reaching -29.75% and 41.2%, respectively. These findings contribute to a deeper understanding of the hydraulic dynamics in hydropower systems and inform decision-making for optimizing system performance.

11 DECLARATION OF INTEREST

The authors declare that the work reported in this paper has not been influenced by competing financial interests or personal relationships.

12 REFERENCES

Elbashir, M., and Amoah, S., 2007. Hydraulic transient in a pipeline (using a computer model to calculate and simulate transient).

Batterton, S. H., 2006. Water hammer: An analysis of plumbing systems, intrusion, and pump operation. Virginia Tech.

Choon, T. W., et al., 2012. Investigation of water hammer effect through the pipeline system. *Journal of Fluids and Structures, 2*(3), 246-251.

Su, C.-K., et al., 2003. Cavitation luminescence in a water hammer: Upscaling sonoluminescence. *Journal of Fluids Engineering, 15*(6), 1457-1461.

Wood, D. J., 2005. Water hammer analysis—essential and easy (and efficient). *Journal of Environmental Engineering, 131*(8), 1123-1131.

Jalut, Q. H., and Ikheneifer, A. A., 2010. Mathematical simulation for transient flow in a pipe under potential water hammer. *Journal of Environmental Systems, 29*(2), 222-236.

Yu, X., Zhang, J., and Miao, D., 2015. Innovative closure law for pump turbines and field test verification. *Journal of Hydraulic Engineering, 141*(3), 05014010.

Wylie, E. B., Streeter, V. L., and Suo, L., 1993. Fluid transients in systems (Vol. 1). Prentice Hall Englewood Cliffs, NJ.

Wan, W., and Zhang, B., 2018. Investigation of water hammer protection in water supply pipeline systems using an intelligent self-controlled surge tank. *Journal of Environmental Engineering, 11*(6), 1450.

Wan, W., et al., 2019. Water hammer control analysis of an intelligent surge tank with spring self-adaptive auxiliary control system. *Journal of Environmental Engineering, 12*(13), 2527.

Triki, A., 2016. Water-hammer control in pressurized-pipe flow using an in-line polymeric short-section. *Applied Mathematics, 227*(3), 777-793.

Vereide, K., et al., 2016. The effect of surge tank throttling on governor stability, power control, and hydraulic transients in hydropower plants. *Energy, 32*(1), 91-98.

Ghidaoui, M. S., et al., 2005. A review of water hammer theory and practice. *Journal of Hydraulic Research, 58*(1), 49-76.

Chaudhry, M., and Hussaini, M., 1985. Second-order accurate, explicit finite-difference schemes for water hammer analysis.

Triki, A., 2017. Further investigation on the resonance of free-surface waves provoked by floodgate maneuvers: Negative surge waves. *Journal of Ocean Engineering, 133*, 133-141.

Triki, A., 2014. Resonance of free-surface waves provoked by floodgate maneuvers. *Journal of Hydrodynamics, 19*(6), 1124-1130.

Triki, A., 2013. A finite element solution of the unidimensional shallow-water equation. *Applied Mathematics, 80*(2).

Karney, B. W., and McInnis, D., 1992. Efficient calculation of transient flow in simple pipe networks. *Journal of Hydraulic Engineering, 118*(7), 1014-1030.

Fang, H., et al., 2008. Basic modeling and simulation tool for analysis of hydraulic transients in hydroelectric power plants. *Journal of Renewable and Sustainable Energy, 23*(3), 834-841.

Zhou, J., et al., 2017. Optimizing guide vane closing schemes of pumped storage hydro unit using an enhanced multi-objective gravitational search algorithm. *Energy Conversion and Management, 10*(7), 911.

Yang, J., et al., 2015. Linear modeling and regulation quality analysis for the hydro-turbine governing system with an open tailrace channel. *Energy, 8*(10), 11702-11717.

Li, H., et al., 2019. Performance evaluation in enabling safety for a hydropower generation system. *Applied Energy, 143*, 1628-1642.

Skulovich, O., et al., 2015. Piecewise mixed integer programming for optimal sizing surge control devices in water distribution systems. *Journal of Water Resources Planning and Management, 51*(6), 4391-4408.

Feng, Z.-k., et al., 2018. Optimization of large-scale hydropower system peak operation with hybrid dynamic programming and domain knowledge. *Renewable Energy, 171*, 390-402.

Connell, D., 2001. Hazen-Williams C-factor assessment in an operational irrigation pipeline.